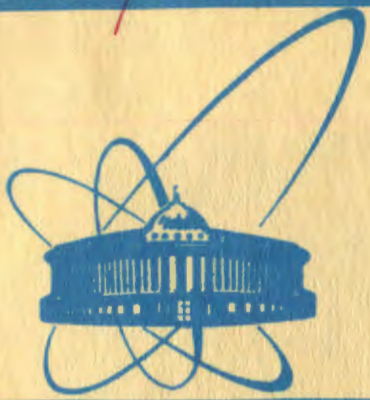

сообщения
объединенного
института
ядерных
исследований
дубна

E1-81-803

W.Peryt, J.Pluta,* T.Pawlak, Z.Strugalski,
V.D.Toneev

COMPARISON OF PREDICTIONS PROVIDED BY THE INTRANUCLEAR-CASCADE MODEL WITH EXPERIMENTAL DATA OBTAINED IN STUDYING PION-XENON NUCLEUS INTERACTIONS AT 3.5 GeV/c MOMENTUM

* Institute of Physics of the Warsaw Technical University, Warsaw, Poland.

1981

1. INTRODUCTION

This article sets out to describe some of the results which have been obtained in our studies of the pion-xenon nucleus collisions. While this work is intended primarily for the elucidation the mechanism of the hadron-nucleus high energy collision process, it is hoped that the information how it is possible to study the hadron-nucleon interaction process using nuclear targets might arise as well.

Commonly known opinion exists that careful and accurate study of the properties of high energy hadron-nucleus collisions can throw light on various aspects of hadronic interactions; indeed, information about various features of the particle-particle interaction is only accessible on this way [1-3].

But, it is clear that before many properties of the hadron-nucleon collision process can be analysed using target-nuclei, an understanding of the hadron-nucleus collision process must be achieved [3]. This was the cause for which we started out investigations of the simplest case of such process under strictly definite initial conditions; the pion-nucleus collisions were investigated using the 180 litre xenon bubble chamber as such track detector which might give the mostly full experimental information [4]. The chamber should be exposed to the pion beam of that energy at which almost all the secondaries emerged in any hadron-nucleus collision could be registered completely through the total solid angle. We applied therefore the beam of negatively charged pions of 3.5 GeV/c momentum.

As currently is practiced, in absence of the strong interaction theory, various models of high energy hadron-nucleus collisions are applied in attempts to explain the experimental data [5-12]. We do not intend to consider many of these models in this paper in connection with our experimental data; we restrict ourselves here to the confrontation of the experimental data to the intranuclear cascade model only, in its version worked out in the Joint Institute for Nuclear Research at Dubna. This model [6,13,14] allows one to predict all the characteristics of the secondaries appearing in pion-xenon nucleus collisions investigated in our experiment. We were able to take into account in this model the conditions of our

experiment in calculating the characteristics which have had to be comparable with the corresponding experimental ones[15].

This paper is arranged as follows: after a short introduction given in section one, we describe our experiment in section two, and we characterize shortly the model used in data analysis in section three; in section four the comparison procedure is shortly described; in section five the comparison of the experimental data with corresponding predictions is presented; the concluding section six contains the discussion of the results arising from our investigations.

2. EXPERIMENT

The hadron-nucleus collision events used for this analysis were registered in the 180-litre xenon bubble chamber[4]. This chamber is built as the rectangular parallelepiped of 104x 40x43 cm^3 volume, without magnetic field.

2.1. Beam and Exposure

The chamber was exposed to negatively charged pion beam of 3.5 GeV/c momentum. During the exposure time no more than five pions were introduced into the chamber, along its length perpendicular to the front wall. The beam pion courses were parallel and widely spreaded within a distance limits of a few centimeters from the chamber axis. Such exposure conditions were of great convenience in studying the pion-xenon nucleus collision events, as we shall see later.

2.2. Scanning and Measurement

The photographs of the chamber were carefully scanned and rescanned for the pion-xenon nucleus collision events which could occur in a chosen parallelepipedal region of nearly 42x10x10 cm^3 volume situated coaxially and centred inside the chamber.

Any sharp change in the straight line track of any beam pion was considered as an indication that this pion undergoes the collision with the xenon nucleus. The end or deflection point of any beam pion track we accepted to be the pion-xenon nucleus interaction location. In fact we were able to detect the collision events in which the beam pion track ends off or deflects at an angle of no less than 2 degrees, in accompaniment or not by any number of tracks outgoing from the interaction plane.

The secondary neutral pions of any kinetic energy, including zero, are recorded and identified in our chamber by the simply visible tracks of the negaton-positon conversion pairs and by the observed electron-photon showers created by the gamma quanta appearing in the neutral pion decay process. The minimum energy of the gamma quanta detected with the constant efficiency amounts nearly 5 MeV. The positive pions stopped within the chamber are identified simply by the characteristic track sequence left by the charged secondaries emerged in the decay process. We meet some difficulties in attempts to identify the negative pions stopping inside the chamber, namely - to distinct them from the stopping protons. But, we estimate, as we shall see later, the content of the stopping pion tracks in the sample of tracks accepted as being left by the stopping protons. Stopping kaons are identified without difficulties as well. Similarly, we can identify hyperons if they decay inside the chamber. The neutrons which are emitted in the collision process interact with the xenon nuclei frequently, leaving characteristic "neutral stars".

Tracks of the length larger than nearly 5 mm are visible well and detectable with the constant efficiency which is close to 100%. To this minimum length there corresponds the minimum kinetic energy of the registered protons of nearly 20 MeV and of the registered charged pions of nearly 10 MeV. The tracks of smaller lengths are visible as well, but in this case the detection efficiency is not constant. The protons of energies from nearly 20 up to nearly 200 MeV, the secondary pions: the negatively charged of kinetic energies from nearly 10 up to nearly 100 MeV, positively charged of kinetic energy from 0 up to nearly 100 MeV, and the neutral pions of any kinetic energy, including 0 MeV, are recorded with the efficiency being near to 100% within the total 4π solid angle. The kinetic energy of protons emitted within the 60 degrees cone and stopping inside the chamber is no more than nearly 350MeV.

The scanning efficiency for all pion-xenon nucleus collision events registered in our experiment was better than 99.5%. In nearly 6% of the registered events the tracks of stopped negative charge pions were indistinguishable from those of the proton tracks; it amounts roughly 2% of all the proton tracks. This estimation follows from the analysis based on the experimental data from the studies of nuclear collisions in nuclear emulsions exposed to the negative pion beam[16]. The contamination of the sample of all the tracks considered to be left by protons by the tracks of deuterons, tritons, and alpha particles was estimated to be no larger than 10%. But, in the majoprity of cases, the tracks of such heavy particles are

shorter than 5 mm; in this experiment we analyse the particles which leave tracks longer than 5 mm.

The accuracy of the proton energy measurement, using the range-energy relation, is 10% for the protons of 15 MeV kinetic energy and for those of 200 MeV kinetic energy[17]. The proton emission angles were measured with an accuracy of 1-8 degrees. In most cases the average accuracy of the proton energy measurement is roughly 4% and that of the emission angle estimation - nearly 3 degrees. The accuracy of the charged pion energy estimation by this method is almost the same. The accuracy of the neutral pion energy estimation[18] amounts nearly 12%, in average. The accuracy of the pion emission angle estimation, for the charged and neutral pions, is about 1 degree.

We have estimated that about 90% of all emitted protons are stopping inside the chamber.

Thus, the sample of all secondaries may be classified into following groups of particles: a) Charged secondaries stopping inside the chamber without interaction or decay; we consider them to be protons. b) Charged secondaries interacting within the chamber or having left it; we accept them to be charged pions. c) Positive pions stopping inside the chamber. d) Neutral pions or eta particles decaying into gamma quanta, causing simply observed negaton-positon pairs or initiating well visible electron-photon showers.

The particles from the groups a)-c) form the class of the charged secondaries the multiplicity of which we denote by N_{ch}. However, we should note that among the particles in the group a) there are (1-2)% admixture of the negatively charged pions and nearly 10% admixture of the heavier particles[6,19]. Similarly, in the group b) an admixture of nearly (10-20)% of protons may be found.

A sample of 2800 pion-xenon nucleus collision events with any number of secondaries were selected in scanning of 25000 chamber photographs. Various experimental characteristics are presented in section 4, and compared with appropriate results predicted by the intranuclear cascade model.

3. INTRANUCLEAR CASCADE MODEL

The cascade approach to nuclear reactions is based on an analogy between the inelastic hadron-nucleus collisions and the transport of a high energy radiation through a block of matter. Both processes are described by the linearized Boltzmann-type equations[6,20]. This analogy enables us to apply the Monte-Carlo method for the analysis of the hadron-nucleus interactions without a direct reference to primary equations[6,21]

In this work we use the Dubna version of the intranuclear cascade model [6,13,14].

The target-nucleus is considered as the Fermi gas of nucleons confined in the potential wall. The diffusive region of the nucleon density distribution and of the nuclear potential is taken into account. The pion-nucleus interaction potential was taken to be equal to 25 MeV, being independent of the pion energy. The influence of the target-nucleus on the intranuclear collisions is limited to the effects of Fermi's motion and Pauli's exclusion principle.

The intranuclear cascade model is based on two general physical assumptions: 1) The projectile particle energy is high enough to be possible to limit ourselves to consider the two-body quasifree collision of this projectile with a nucleon inside the target-nucleus. 2) The hadron-nucleon interaction time is much shorter than the average time interval between the subsequent hadron-nucleon collisions which allows one to assume that the colliding particles approach their normal state before to come again into collision.

Under such conditions the projectile high energy hadron starts the intranuclear cascade of subsequent fast particle collisions, in colliding with the target-nucleus. The behaviour of each of the cascade particles is described by the linearized Boltzmann-type equation. This linearization is achieved, if interaction between the cascade particles is not taken into account, i.e., the cascade particles are considered to be of some kind of the ideal gas of nucleons and pions.

The hadron-nucleon elementary collisions were simulated by the statistical method [6,13] in which available data from the experimental studies of such reaction were used. The pion production process was taken into account. The energy-momentum conservation law was ordered to be fulfilled in any simulated elementary interaction act. To what extent the main characteristics of the secondaries agree with the experimental ones is discussed in detail earlier [6,13]. The comparison of predictions of the Dubna version of the intranuclear cascade model with other ones, at energies of the projectile-hadron when the pion creation process can be neglected, is presented in the collaboration paper [22].

The important process which is taken into account in our version of the intranuclear cascade model is the secondary pion absorption by two nucleon associations in the target-nucleus. The change of the nucleon density inside the target in developing the cascade is taken into account [14,23]. It allows one to reproduce the saturation effect in the energy dependence of average multiplicities of grey and black tracks at kine-

tic energies $T_0 \geq 3$-5 GeV, observed in the emulsion experiments, and therefore to extend the applicability of the model up to projectile energies of 20-30 GeV [14].

In treating the second stage of the hadron-nucleus collision process, the slow one, the calculations are based on the equilibrium statistical theory (in evaporation approximation). The processes of the nucleon, deuteron, triton, ^{3}He nucleus, and alpha particle emission were taken into account [6]. It is found to be needed to stress out that all the calculations were performed in the framework of the standard statistical cascade model without attempts to fit it to the experimental data.

4. THE COMPARISON PROCEDURE

For a comparison of the experimental data with the predictions of the intranuclear cascade model, 7626 random "stars" were generated. These simulated events were transformed to the registration conditions existing in our chamber and recorded on the magnetic type; in transformation the limited volume of the chamber was taken into account. In particular, every collison event constructed in the simulation procedure was taken to occur within the chamber region which was accepted as the location of the interactions in the experiment.

The next step was to determine the behaviour of each charged secondary in the simulated collision event, when it would occur in the chamber. When the charged secondary was found to be stopping it was qualified to be belonging to the group a), corresponding to appropriate group of the events registered in experiment; when it was found not the case, the secondary was qualified to be belonging to corresponding group b) - to the charged secondaries escaping the chamber. If the secondary was qualified to be belonging to the group a), but it was identified to be pion, the correction was introduced: it was considered to be proton, according to the scanning conditions in the experiment, and corresponding value of kinetic energy was estimated for this "proton". Such procedure, according to the registration and identification conditions in the experiment, makes the experimental verification of the model to be precise. The characteristics of the simulated events produced in such a way correspond to appropriate characteristics of the events registered in the experiment. The data processing of both the samples of events, the real and the simulated ones, was realized separately by applying the same programme library.

To end this section, we quote the particle composition in the classes a) and b) in the sample of simulated events. Among

the particles stopping inside the chamber the group a) - the protons - amounts the predominant component, 82.7%; the admixture of negative pions in this group is 16.4%, those of remaining 0.9% belong to heavier particles. Among the secondaries qualified to be belonging to the group b) the negative pions amount 24.8% and the fast protons are in 25.4%.

5. RESULTS

General characteristics of the data which have to be discussed later, of both - the simulated by using the intranuclear cascade model and the experimental ones, are presented in table 1. We start the presentation of these data with the multiplicity distributions of various secondaries.

5.1. Multiplicity Distributions of Secondary Particles

The emission intensity of the secondaries seems to be one of essential characteristics of the hadron-nucleus collision process. As usually is practiced, as a characteristic of the intensity of emitted protons the proton multiplicity distribution of the collision events is presented; the multiparticle production process is characterized by the secondary pion multiplicity distributions. In figs. 1-3 appropriate characteristics are given, both - the experimental and the predicted ones.

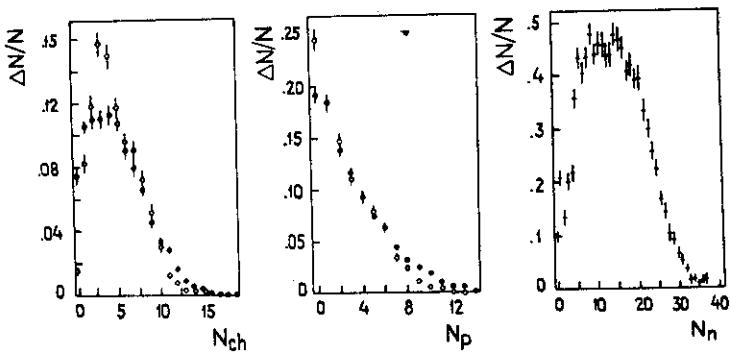

Fig.1. Multiplicity distributions of various secondaries in pion-xenon nucleus collisions at 3.5 GeV/c momentum. N_{ch} - charged secondary multiplicity, N_n - neutron multiplicity, N_p - proton multiplicity. o - experimental data, • and + - predictions of the cascade model.

Table 1

General characteristics of the data, of both - the experimental and the simulated applying the intranuclear cascade model, used in the study of the pion-xenon nucleus collisions at 3.5 GeV/c momentum:

a) The characteristics of the total number of 7626 simulated events; the conditions of the experiment are not taken into account

Secondary particle	Number of particles	Average number of secondaries per event
Any charged	70456	9.24 ± 0.07
Protons	36856	4.83 ± 0.04
Negative charge pions	12442	1.63 ± 0.01
Positive charge pions	5605	0.74 ± 0.01
Neutral pions	11337	1.48 ± 0.01
Neutrons	109598	14.37 ± 0.08
Deuterons	5712	0.75 ± 0.01
Tritons	2775	0.36 ± 0.01
^{3}He nuclei	666	0.09 ± 0.04
Alpha particles	6400	0.84 ± 0.01

b) The characteristics of the sample of the simulated collision events, when the experimental conditions of the secondary registration were taken into account; for the comparison appropriate experimental data are presented as well.

Secondary particle	Model		Experiment	
	Number of secondaries	Average number of secondaries per event	Number of secondaries	Average number of secondaries per event
Protons	23995	3.13 ± 0.03	7250	3.01 ± 0.04
Stopping positive pions	2040	0.27 ± 0.03	271	0.10 ± 0.01
Escaping charged pions	10514	1.38 ± 0.01	-	-
Blobs (track smaller 5 mm)	33907	4.45 ± 0.05	2657	0.95 ± 0.05
All charged	-	-	16044	5.74 ± 0.11
V^0	-	-	176	0.06 ± 0.05

c) The percentage of various secondary particles in pion-xenon collision events, estimated by using the model, for various groups: "protons", "blobs", "escaping" for which the secondaries are qualified in the experiment.

The groups of secondaries					
"Protons"		"Escaping"		"Blobs"	
Particles	%	Particles	%	Particles	%
Protons	82.7	Protons	25.4	Protons	42.3
Negative pions	16.4	Negative pions	49.8	Negative pions	9.7
Others	0.9	Positive pions	24.8	Positive pions	2.8
-	-	-	-	^{3}He	2.0
-	-	-	-	Deuterons	16.5
-	-	-	-	Tritons	8.1
-	-	-	-	Alpha particles	18.6

Table 2

Average multiplicities of secondaries, r.m.s., and skewness.

The multiplicity of secondaries	Experiment			Model		
	a_1	a_2	a_3	a_1	a_2	a_3
N_{ch}	4.79 ± 0.05	2.70	0.56	4.79 ± 0.04	3.30	0.60
N_p	2.59 ± 0.05	2.47	0.96	3.12 ± 0.03	2.89	1.04
$N_{\pi^\pm}$	3.02 ± 0.03	1.44	0.50	3.13 ± 0.02	1.83	0.16
$N_{\pi^\pm}$	2.08 ± 0.03	1.26	0.56	1.65 ± 0.02	1.35	0.67
N_{π°	0.94 ± 0.02	0.99	1.14	1.49 ± 0.01	1.20	0.66

Designations: N_{ch} - charged secondary multiplicity; N_π - pion multiplicity; N_p - proton multiplicity. a_1 - average value; a_2 - r.m.s.; a_3 - skewness.

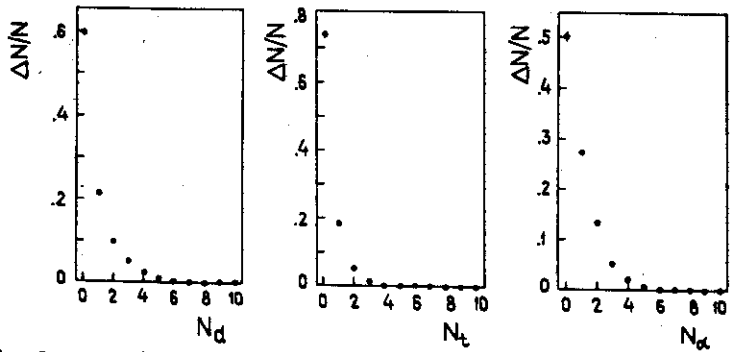

Fig.2. Multiplicity distributions of emitted nuclei, predicted by the intranuclear cascade model. N_d - deuteron multiplicity, N_t - triton multiplicity, N_α - alpha particle multiplicity.

It can be seen that the calculated average multiplicity of the charged secondaries $\langle N_{ch} \rangle$ is in agreement with the experimental one, table 2; but, the shapes of the charged secondary multiplicity distributions differs evidently, fig.1. The experimentally estimated proton average multiplicity $\langle N_p \rangle$ differs from the predicted one, table 2. From fig.1 we see that the number of events with the proton multiplicity $N_p=0$, predicted by the model, is nearly of 20% smaller than it is observed in experiment. Another interesting feature seems to be a large excess in the calculated neutral pion multiplicity:

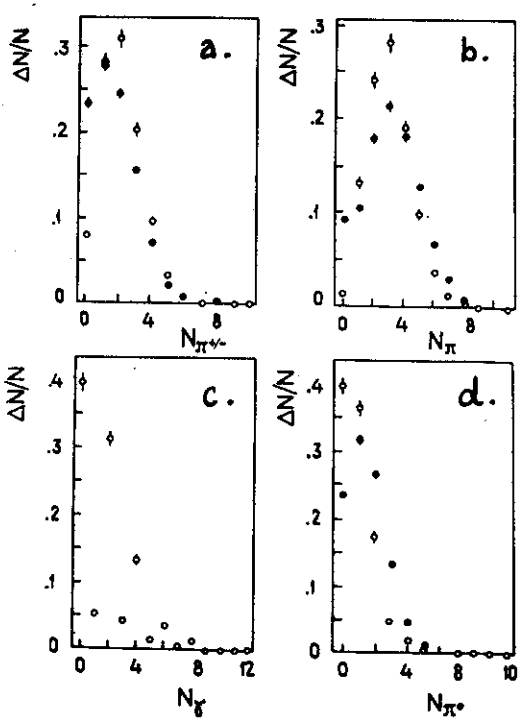

Fig.3. Multiplicity distributions of: a)charged pions, b)any charge pions, c)gamma quanta, d)neutral pions. • - predicted by the model, o - experiment.

$(\langle N_{\pi^0}^{mod} \rangle - \langle N_{\pi^0}^{exp} \rangle)/\langle N_{\pi^0}^{exp} \rangle = 0.5$. The average multiplicity of the charged secondary pions $\langle N_{\pi^\pm} \rangle$ observed in experiment is, in contrary, larger than those prediced by the model, table 2. But, the average multiplicity of all the secondary pions $\langle N_{\pi^\pm, \pi^0} \rangle$ is reproduced by the model quite well, table 2.

5.2. Angular Distribution of Secondaries

The angular characteristics of the proton emission and pion creation are shown in fig.4. Both the series of characte-

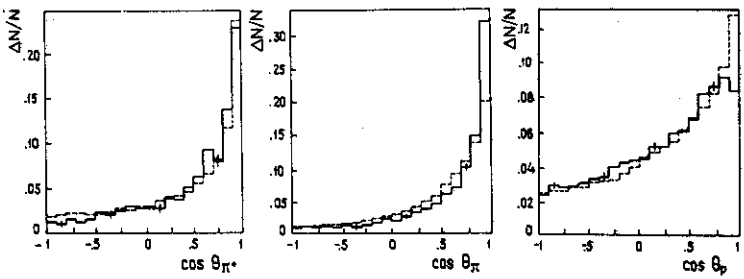

Fig.4. Angular distributions of: neutral pions, all secondary pions, protons. The emission angle; ——— experiment, ----- model

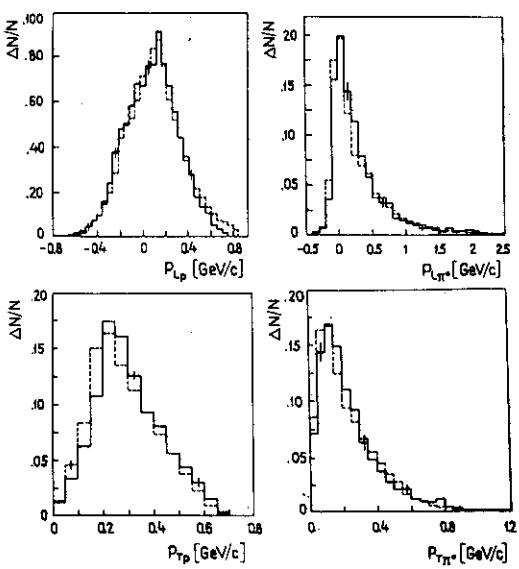

ristics, the experimental and the predicted ones, differ within the secondary emission angle values θ_p and θ_π: $0.9 < \cos\theta < 1.0$; for the neutral pions such difference is not observed at all.

Fig.5. The spectra of the longitudinal P_L and transversal P_T momenta of protons and neutral pions; solid line - experimental data, dotted line - predictions by the model.

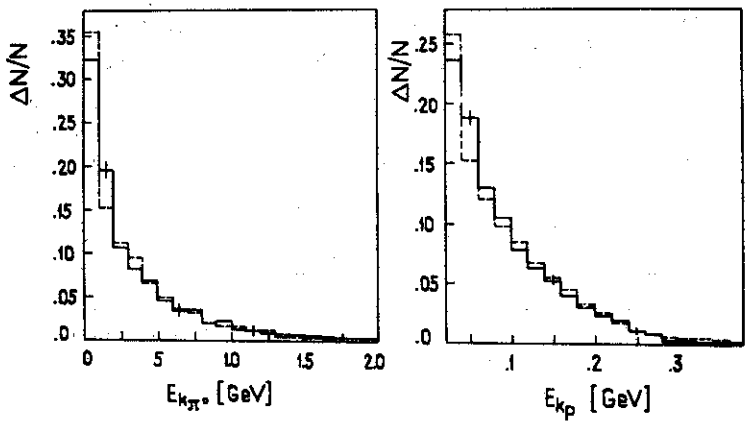

Fig.6. Kinetic energy spectra of the neutral pions and protons; solid line - experiment, dotted line - predictions.

5.3. Momentum and Energy Distributions of the Secondaries

The longitudinal P_L and transversal P_T momentum spectra of the emitted protons and produced neutral pions are shown in fig.5. The energy spectra are shown in fig.6.

5.4. Correlations between Various Characteristics of Secondary Particle Emission

The correlations between various quantities characterizing the secondaries emitted in hadron-nucleus collisions might provide important information about the collision process. The correlations were studied between: a) the average proton multiplicities $\langle N_p \rangle$ and the charged secondary multiplicities N_{ch} and secondary pion multiplicities N_π, fig.7; b) the average multiplicities of various pions - neutral $\langle N_{\pi^0} \rangle$ and charged $\langle N_{\pi^\pm} \rangle$, and the proton multiplicity N_p or the charged pion multiplicity N_π, fig.8; c)the average cosine of the meson emission angle θ_π or the average cosine of the proton emission angle θ_p, and the proton or pion multiplicity, fig.9; d)the average transversal $\langle P_T \rangle$ momenta of the secondary neutral pions or the emitted protons and the proton multiplicities N_p, fig.10; e) the average transversal momentum of the neutral pions $\langle P_{T\pi^0} \rangle$ and corresponding longitudinal momentum $P^*_{L\pi^0}$, fig.11.

The intranuclear cascade model reflects the behaviour of the above presented correlation characteristics, but it should

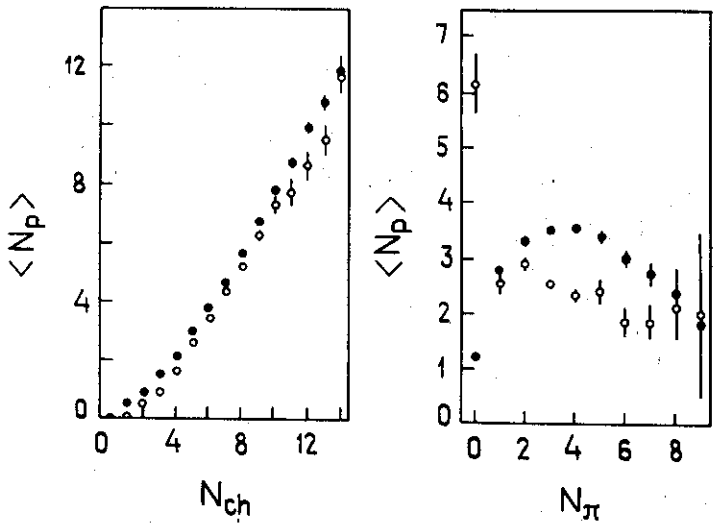

Fig.7. Correlations between the average proton multiplicity $\langle N_p \rangle$ and the charged secondary multiplicity N_{ch} and the secondary pion multiplicity N_π. ● - model, ○ - experiment.

be stressed out the existence of evident disagreements between the predictions and the experimental data, when as the variables the multiplicities are taken of the secondaries which experimental characteristics are in disagreement with corresponding predictions, as it has been shown in section 5.1.

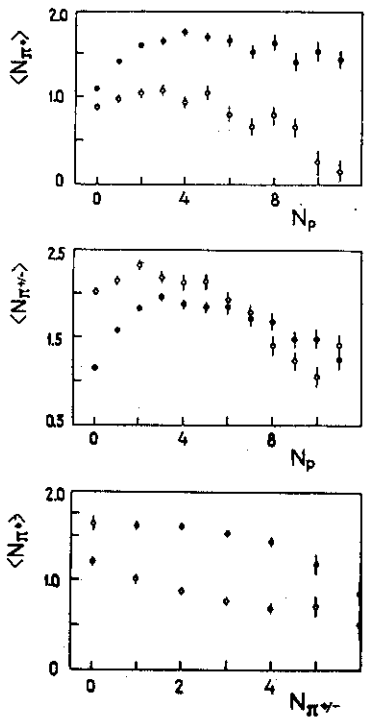

Fig.8. The dependences of the average multiplicities of the neutral pions $\langle N_{\pi^0} \rangle$ and charged pions $\langle N_{\pi^\pm} \rangle$ on the proton multiplicity N_p, and the dependence of the neutral pion average multiplicity on the charged pion multiplicity $N_{\pi^\pm}$: ○ - experiment, ● - model.

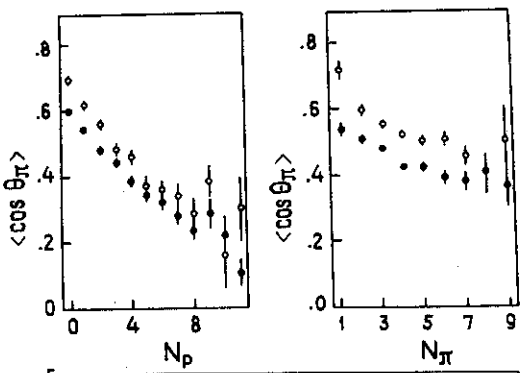

Fig.9. Correlations between the average angles $\langle\cos\theta\rangle$ of the secondary emission and the secondary multiplicity N. o - experiment, • - model.

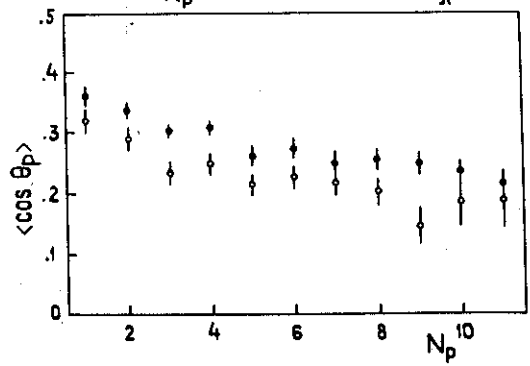

Fig.10. Average momenta $\langle P_p\rangle$ and average transversal momenta $\langle P_{Tp}\rangle$ of the emitted protons, and average transversal momenta $\langle P_{T\pi^0}\rangle$ of the produced neutral pions in dependence on the proton multiplicity N_p ; o - experiment, • - model.

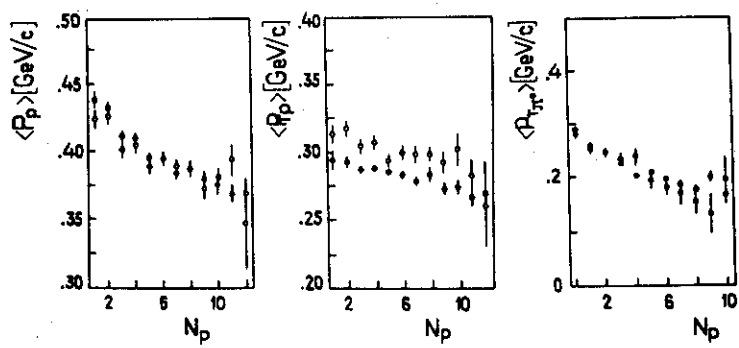

6. Conclusions

The purpose of this work was to study pion-nucleus interactions at a few GeV energy. The experimental part is based on the mostly full information, obtained from the pion-xenon nucleus collision studies using 180 litre xenon bubble chamber exposed to 3.5 GeV/c momentum pions of negative electric charge.

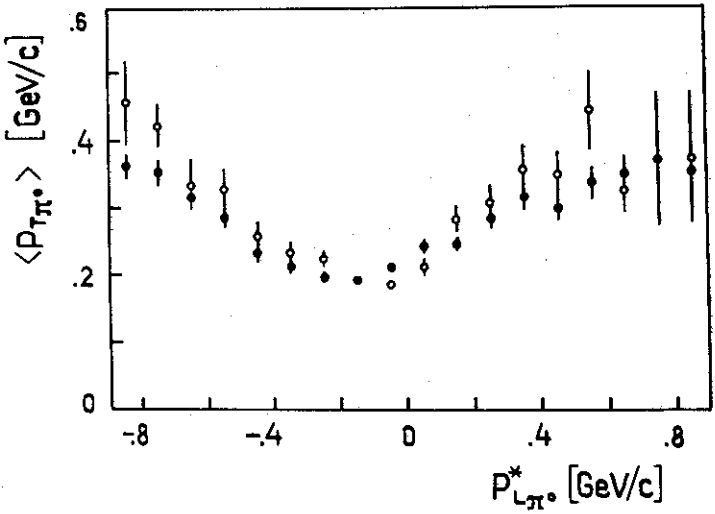

Fig.11. Correlations between the average transversal momentum $\langle P_{T\pi^0} \rangle$ of secondary neutral pions and the c.m.s. longitudinal momentum of these pions $P^*_{L\pi^0}$; o - experiment, ● - model.

As theoretical basis for the comparative analysis the intranuclear cascade model, in such conditions which correspond strictly to observation and registration conditions of the collision events and the secondaries appearing in them in the experiment, has been used. In particular, full information about the neutral pions ejected in pion-nucleus collisions was given in our experiment, the size of the chamber was taken into account in calculations being performed according to the intranuclear cascade model. Therefore, the results of our experiment and corresponding predictions given by the model were just applicable for a comparison.

As the conclusion from the comparison of the experimental results with corresponding predictions, we can state:

1. The multiplicity distributions of the secondaries given by experiment are reproduced well enough at higher multiplicity values, fig.1 and fig.3. Various levels of this agreement are observed for various secondaries: protons, charged pions, and neutral pions. Disagreement is evidently seen at small values of the secondary multiplicities.
2. The angular distributions of secondary pions and protons, both the experimental and the predicted ones, are of nearly the same shapes, but evident disagreement is seen at small angle values, fig.4.

3. Momentum and energy distributions of the secondaries provided by the experiment agree well enough with the predicted by the model, fig.5 and fig.6.
4. Correlations between various characteristics of the secondary particle emission process provided by the experiment differ from the predicted ones, figs.7-11, although, in many cases, we observe similar shapes of the characteristics, fig.9, fig.10, fig.11.

In result of the investigations which we have spoken above about, we can state that the discussed version of the intranuclear cascade model can serve for a preliminary estimation of various characteristics of the hadron-nucleus collision process at incident hadron energies of a few GeV.

But, some important features are not reproduced correctly by this model. The question arises here: whether the discrepances are due to shortcomings of the given version of the intranuclear cascade model or they are a manifestation of other possible nature. In this relation, a comprehensive comparison of a large body of now available experimental data with different theoretical models is of great interest.

REFERENCES

1. Blin-Stoyle R.J. Contemporary Physics, 1979, 20, p. 377.
2. High Energy Physics and Nuclear Structure, Santa-Fe and Los Alamos, AIP Conf.Proc., 1975, No. 26.
3. Busza W. Acta Physica Polonica, 1977, B8, p. 333.
4. Kusnetsov E.V., et al. Instr. and Experimental Technique (Russian PTE), 1970, B8, p. 333.
5. Miesowicz M. Progress in Elementary Particle and Cosmic Ray Physics, 1971, 10, p. 128.
6. Barashenkov V.S. Toneev V.D. Interactions of High Energy Particles and Nuclei with Nuclei, Atomizdat, Moscow, 1972.
7. Friedländer E.M. Lett. Nuovo Cimento, 1974, 9, p. 349..
8. Claucci J. Phys.Rev., 1974, D10, p. 1468.
9. Zalewski K. Topical Meeting on Multiparticle Production at Very High Energies, Trieste, 1976.
10. Florian J.R. et al. Phys.Rev., 1976, D13, p. 558.
11. Brodsky K. et al. Phys.Rev.Lett., 1977, 39, p. 1120.
12. Babecki J., Nowak G. Acta Phys.Polonica, 1979, B10, p.705.
13. Barashenkov V.S., Gudima K.K., Toneev V.D. Acta Physica Polonica, 1969, 36, p. 415, 457, 887.
14. Barashenkov V.S., Ilinov A.S., Toneev V.D. Journ. of Nuclear Physics (Russian), 1971, 13, p. 743.

15. Peryt W. Analysis of the High Energy Pion-Xenon Nucleus Collisions Using Characteristics of the Neutral Pions Produced, PhD Thesis Institute of Physics, Warsaw Technical University, Warsaw, Poland, 1979.
16. Menon M.G.K., Muirhead H. Rochot O. Phil.Mag., 1950, 41, p. 583.
17. Kanarek T., Strugalski Z. JINR, 1-3320, Dubna, 1967.
18. Strugalski Z. JINR, 796, Dubna, 1961; Konovalova L.P., Okhrimenko L.S., Strugalski Z. Instrumentation and Experimental Technique (Russian PTE), 1961, 6, p. 26; Ivanovskaya I.A. et al. PTE,1968, 2, p. 39; Strugalski Z. JINR, P13-6406, Dubna, 1972.
19. Powell C.F., Fowler P.M., Perkins D.H. Study of the Elementary Particles by the Photographic Methods, London-N. York-Paris-Los Angeles, 1959; Bayukov J.D. et al. Journal of Nuclear Research (Russian), 1973, 18, p. 1246.
20. Goldberg M., Wattson K. Theory of Collisions, "Mir", Moscow, 1967.
21. Serber R. Phys.Rev., 1947, 72, p. 1114.
22. Barachenkov V.S. et al.Nuclear Phys., 1972, A187, p. 531.
23. Barashenkov V.S. et al. Uspekhy Fiz. Nauk, 1973, 109, p.91.

Received by Publishing Department
on Department 17 1981.